# Germanate Anomaly and Its Temperature Dependence: An Ultra-high field 17O NMR Spectroscopic Study of Sodium Germanate Glasses

<sup>1</sup>Sabyasachi Sen, <sup>2</sup>Jonathan F. Stebbins, <sup>3</sup>Yijue Xu, <sup>3</sup>Ivan Hung, <sup>3</sup>Zhehong Gan

<sup>&</sup>lt;sup>1</sup>Department of Materials Science and Engineering, University of California at Davis, Davis, California 95616, USA

<sup>&</sup>lt;sup>2</sup>Department of Earth and Planetary Sciences, Stanford University, Stanford, California 94305, USA

<sup>&</sup>lt;sup>3</sup>National High Magnetic Field Laboratory, 1800 East Paul Dirac Drive, Tallahassee, Florida 32310, USA

#### **Abstract**

The oxygen speciation in  $(Na_2O)_x(GeO_2)_{I00-x}$  glasses with  $4 \le x \le 28$  is studied using high-resolution  $^{17}O$  NMR spectroscopy at ultra-high field (35.2 T). The structure of glasses with  $x \le 18$  consists of oxygen atoms bridging either two four-coordinated  $Ge^{IV}$  atoms  $(O^{44})$  or a  $Ge^{IV}$  and another six-coordinated  $Ge^{VI}$  atom  $(O^{46})$ . The  $O^{46}$ :  $O^{44}$  ratio monotonically increases with increasing  $Na_2O$  content in this composition range. Further addition of  $Na_2O$  results in a lowering of  $O^{46}$  and in a concomitant rise in the concentration of non-bridging oxygen (NBO) atoms. The resulting compositional variation in the average coordination number of Ge atoms is associated with the non-monotonic evolution of density and the germanate anomaly in these glasses. On the other hand, increasing fictive temperature results in a net conversion of  $Ge^{VI} \rightarrow Ge^{IV} + NBO$  in these glasses, which is argued to be a source of temperature dependent configurational entropy in germanate liquids.

#### 1. Introduction

The incorporation of an oxide ion into the structure of silicate or phosphate glasses via the addition of a modifier oxide to SiO<sub>2</sub> or P<sub>2</sub>O<sub>5</sub> results in the formation of non-bridging oxygen (NBO) atoms that lower the connectivity of the network [1,2]. On the other hand, the borate and germanate networks respond quite differently as the coordination number of B and Ge cations increases upon initial addition of oxide ions and consequently the connectivity of the network increases [3]. Specifically, in borates, some four-coordinated boron begins to form from trigonal groups, and in germanates some five-or six-coordinated Ge begins to form from tetrahedral species. The conversion of 4-fold coordinated Ge<sup>IV</sup> atoms to 5-fold and 6-fold coordination (Ge<sup>V</sup> and Ge<sup>VI</sup>, respectively) can be expressed in the form of structural reactions such as [4]:

$$M_2 O + Ge^{IV} \emptyset_{4/2} \to \left[ Ge^{VI} \emptyset_{6/2} \right]^{2-} + 2M^+$$
 (1)

$$M_2 O + 2 G e^{IV} \emptyset_{4/2} \rightarrow 2 [G e^V \emptyset_{5/2}]^- + 2M^+$$
 (2)

In these reactions  $\emptyset$  and  $O^-$  represent bridging and non-bridging oxygen atoms, respectively, and  $M^+$  is a modifier cation.

In the case of alkali germanates, the concentration of high-coordinated Ge is maximized at an alkali oxide concentration of ~ 15-20 mol%, beyond which further addition of alkali oxide results in the lowering of the relative fraction of the high-coordinated Ge and a concomitant increase in the NBO content [5,6]. This structural change can be represented via reactions such as [5]:

$$\left[Ge^{VI} \phi_{6/2}\right]^{2^{-}} + 2M^{+} + Ge^{IV} \phi_{4/2} \to 2(Ge^{IV} \phi_{3/2} O^{-}.M^{+})$$
(3)

At this point, similar to silicates and phosphates, the connectivity of the germanate network starts to decrease. This compositional evolution of the network is believed to give rise to the so-called

"germanate anomaly", where the density and the glass transition temperature  $T_g$  of alkali germanate glasses display a non-monotonic variation with the modifier content and go through a maximum at an alkali oxide content where the concentration of the high-coordinated Ge also maximizes [4-8]. Previous structural studies of alkali germanate glasses employed Raman spectroscopy, X-ray and neutron scattering and Ge extended x-ray absorption fine structure (EXAFS) spectroscopy, all of which provided clear evidence in favor of an increase followed by a decrease in the average Ge coordination number with the addition of modifier alkali oxide [9-13]. However, the relative abundance of the Ge<sup>V</sup> and Ge<sup>VI</sup> species in these glasses has remained undetermined. A number of these studies have challenged the idea of a sole causal link between the germanate anomaly and the Ge coordination environment [7,14-17]. These studies suggested instead that Ge<sup>V</sup> may the most dominant high-coordinated species in alkali germanate glasses and the germanate anomaly is a consequence of a complex interplay between this species, the formation of NBOs and the appearance of three-membered GeO<sub>4</sub> rings [7]. More recent <sup>17</sup>O triplequantum magic-angle-spinning (3QMAS) nuclear magnetic resonance (NMR) spectroscopic studies of glassy sodium germanates have also provided clear corroborating evidence in favor of an increase in the relative concentration of five- and/or six- coordinated Ge atoms with the addition of up to ~ 20 mol% modifier alkali oxide [4,5]. Further increase in the alkali content was shown to result in the appearance of NBOs in the glass structure and a concomitant lowering of the concentration of high-coordinated Ge atoms. <sup>17</sup>O NMR can potentially provide key information regarding not only the concentration of Ge in different coordination environments but also their connectivity in the network. However, it may be noted that multiple-quantum MAS NMR is inherently a semi-quantitative technique, and "single-quantum" MAS data would be highly desirable for obtaining fully quantitative oxygen speciation in these glasses [4,5].

Finally, the pronounced difference between the compositional variation of the molar volume of sodium germanate glasses and that of the corresponding liquids was suggested in the literature to be indicative of significant temperature dependence of the Ge speciation reactions in Eqs. 1 and 2 [4,14,18]. Temperature is indeed well known to have a significant effect on the coordination of B atoms in oxide glasses/liquids where it has been demonstrated that increasing temperature shifts the speciation equilibrium BO<sub>4</sub>= BO<sub>3</sub>+NBO to the right, with BO<sub>4</sub> and BO<sub>3</sub> being the relative fractions of 4- and 3- coordinated B atoms, respectively [19-25]. Such speciation increases the configurational entropy  $S_{conf}$  of the borate network, and has been linked to viscous flow within the framework of the Adam-Gibbs configurational entropy model [19-21,25,26]. According to this model the temperature dependence of the configurational entropy of a glassforming liquid i.e.  $\frac{dS_{conf}}{dT}$  is proportional to its fragility, which is a measure of the degree of departure of its viscosity from an Arrhenius behavior in the glass transition range. It may be noted here that the fragility of a glass-forming liquid is parameterized by the fragility index m, which is defined as:  $m = \frac{d \log_{10} \eta}{d T_g / T} \Big|_{T=T_o}$  [26]. Indeed, recent high-temperature Raman spectroscopic studies of K<sub>2</sub>O-GeO<sub>2</sub> liquids have hinted that the Ge speciation in these liquids is temperature dependent such that the formation of NBOs is favored with increasing temperature at the expense of the highcoordinated Ge species according to the reaction in Eq. 3 [27].

The temperature dependence of this speciation reaction is indeed consistent with density being related to the Ge coordination and its decrease with increasing temperature is consistent with a concomitant decrease in average Ge-O coordination number. Again, high-resolution <sup>17</sup>O MAS NMR spectroscopy may offer unique and direct element-specific information on the temperature dependent oxygen speciation in these glasses.

However,  $^{17}O$  MAS NMR spectroscopy of alkali germanate glasses has proved to be rather challenging with poor resolution even at magnetic fields of up to 18.8 T, indicating the need for the utilization of even higher magnetic fields where the quadrupolar line broadening effects would be minimized [4,5,28]. It may be noted that for central transition spectra of half-integer quadrupolar nuclides such as  $^{17}O$  broadened by second-order quadrupolar effect, an increase in magnetic field results in an increase in resolution and sensitivity proportional to the square of the magnetic field in ppm scale [29,30]. Here we present high-resolution  $^{17}O$  MAS NMR spectroscopic data on binary Na<sub>2</sub>O-GeO<sub>2</sub> glasses with 4 mol%  $\leq$  Na<sub>2</sub>O  $\leq$  28mol% obtained at an ultra-high magnetic field of 35.2 T. These results are utilized to investigate the compositional evolution of the oxygen speciation and Ge-O coordination as well as their temperature dependence in these glasses.

## 2. Experimental

#### 2.1. Glass synthesis and characterization

 $(Na_2O)_x$  (GeO<sub>2</sub>)<sub>100-x</sub> glasses with x = 4, 8, 18 and 28 were synthesized from <sup>17</sup>O isotope-enriched crystalline trigonal GeO<sub>2</sub> and Na<sub>2</sub>CO<sub>3</sub> by decarbonating the stoichiometric mixtures at 750 °C followed by melting in sealed Pt tubes at 1200 °C for 1h followed by quenching. The <sup>17</sup>O isotope-enriched GeO<sub>2</sub> was obtained by hydrolysis of Ge(OC<sub>2</sub>H<sub>5</sub>)<sub>4</sub> with 76% <sup>17</sup>O-enriched H<sub>2</sub>O followed by heating the product at 350 °C in Ar gas. The details of the hydrolysis procedure can be found in previous studies [4,5]. Samples of "as-quenched" glasses with x = 18 and 28 were annealed at  $T_a = 490$  and 420 °C, respectively, for 7 days to equilibrate these to lower fictive temperatures  $T_f$ . These two glasses are designated as "annealed" in the subsequent discussion and the annealing temperatures  $T_a$  were chosen such that  $T_g/T_a$  were identical ( $T_g/T_a \sim 1.06$ ) for both

compositions. The glass transition temperature for these two glasses with x = 18 and 28 were taken from the literature to be ~ 537 and 463 °C, respectively [8]. Density of all glasses was measured using a gas expansion pycnometer (Micromeritics AccuPyc II 1340) at 20°C using helium (6N purity) as the displacement gas, and for the "as-quenched" samples was found to be consistent the values reported in the literature for comparable compositions [8]. As expected, the density of these glasses goes through a maximum near x = 18. Moreover, the density of the samples with x = 18 and 28 increase upon annealing at temperatures below  $T_g$  for 7 days, indicating a concomitant lowering in  $T_f$ . These density values are shown in Figure 1.

## 2.2. NMR spectroscopy

The  $^{17}O$  MAS NMR spectra of all  $(Na_2O)_x(GeO_2)_{100-x}$  glasses were collected at the National High Magnetic Field Laboratory (NHMFL) using the ultra-high field (35.2 T) series-connected hybrid magnet ( $^{17}O$  resonance frequency 203.4 MHz) using a Bruker Avance NEO console and a 3.2 mm MAS probe designed and constructed at the NHMFL. Crushed glass samples were taken in ZrO<sub>2</sub> rotor and were spun at 16 kHz. The 1D  $^{17}O$  Hahn echo ( $\pi/2$ - $\tau$ - $\pi$ -acq) experiments were recorded by setting the inter-pulse delay  $\tau$  to be equal to 8 rotor periods, and with  $\pi/2$  and  $\pi$  pulse lengths of 6.0 and 12.0  $\mu$ s, respectively. All spectra were collected at ambient temperature with recycle delay of 1s, and 320 to 1080 transients were averaged, and Fourier transformed. A recycle delay of 1s was found to be sufficient as delays longer than 1s did not significantly affect the line shape. The  $^{17}O$  chemical shift for all spectra was referenced externally to distilled H<sub>2</sub>O at 0 ppm.

## 3. Results and Discussion

# 3.1. Compositional evolution of glass structure

The ultra-high field <sup>17</sup>O MAS NMR spectra of all (Na<sub>2</sub>O)<sub>x</sub> (GeO<sub>2</sub>)<sub>100-x</sub> glasses studied here are shown in Figure 2. The  $^{17}O$  MAS NMR spectra of glasses with x  $\leq$ 18 display two resonances centered near  $\sim 50$  and 90 ppm and their associated spinning sidebands. Based on the  $^{17}\mathrm{O}$  chemical shift systematics in alkali germanates established in previous studies, these two resonances can be assigned, respectively, to bridging oxygen in  $Ge^{IV}$ -O- $Ge^{IV}$  (denoted henceforth as  $O^{44}$ ) and  $Ge^{IV}$ -O-Ge<sup>V</sup> or Ge<sup>IV</sup>-O-Ge<sup>VI</sup> (denoted henceforth as O<sup>45</sup> and O<sup>46</sup>) environments [4,5]. These spectra clearly indicate an increase in the relative intensity of the O<sup>45/46</sup> resonance with increasing alkali content in this composition range, implying a corresponding increase in the relative concentration of high-coordinated GeV and/or GeVI species. Besides these two resonances, the <sup>17</sup>O MAS NMR spectrum of the glass with x = 28 (Figure 2) displays an additional partially resolved resonance near ~ 40 ppm, which can be assigned to a NBO environment and a rather weak but well-resolved resonance near ~ 237 ppm, which corresponds to an oxygen bridging three GeO<sub>6</sub> octahedra i.e. an O<sup>666</sup> environment [4]. To the best of our knowledge, this is the first observation of such oxygen environments in alkali germanate glasses. The apparent absence of other three-coordinated oxygen species such as O<sup>466</sup> or O<sup>566</sup> can then be explained using simple bond valence arguments. For example, for an  $O^{666}$  environment each of the three  $Ge^{VI}$  contributes  $+\frac{2}{3}$  charge to the oxygen and thus the total positive charge of +2 is exactly compensated by the -2 charge on the oxygen ion. In contrast, the total positive charge on the oxygen for an O<sup>466</sup> environment would be:  $1 + \frac{2}{3} + \frac{2}{3} =$ 

2.33 and that for an O<sup>566</sup> environment is:  $\frac{4}{5} + \frac{2}{3} + \frac{2}{3} = 2.13$ , either of which would result in an excess positive charge on the oxygen ion, rendering such oxygen species energetically less stable.

Gaussian lines are used to simulate these resonances in the <sup>17</sup>O MAS NMR spectra in Figure 2. It may be noted that the quadrupolar broadening effect on the <sup>17</sup>O NMR line shape is significantly smaller than the broadening induced by chemical shift distribution at such high magnetic fields. For example, for an oxygen environment with a quadrupolar coupling constant  $C_Q$  of 5 MHz, the intrinsic quadrupolar linewidth at this field is only ~ 5 ppm, which is ~ 4x to 10x lower than the full width at half maximum (FWHM) of the constituent <sup>17</sup>O resonances in these germanate glasses (see below), and the latter is thus entirely controlled by the chemical shift distribution. Consequently, these ultra-high field <sup>17</sup>O MAS spectra can be treated as those of spin-1/2 nuclides, which justifies the use of Gaussian lines in these simulations [30]. The simulation parameters and the relative fractions of the various oxygen species as obtained from the peak areas under these resonances are listed in Table 1. The isotropic chemical shifts  $\delta_{iso}$  as well as the relative fractions of these oxygen species are consistent with those estimated from <sup>17</sup>O 3QMAS NMR spectra (Figure 3) in previous studies [4,5]. It may be noted that the  $\delta_{iso}$  for both O<sup>44</sup> and O<sup>45/46</sup> species continuously increase with increasing Na<sub>2</sub>O content in these glasses (Table 1). This trend was attributed in previous studies by Stebbins and coworkers [4] to a lengthening of Ge-O bonds related to the closure of Ge-O-Ge angles due to an increased interaction between the bridging oxygen atoms and the modifier Na cations. On the other hand, the FWHM of the <sup>17</sup>O resonances corresponding to the O<sup>44</sup>, O<sup>45/46</sup> and NBO environments are found to be quite different from one another (Table 1). The FWHM of the  $O^{45/46}$  resonance is the largest (~ 40-45 ppm), while that of the NBO resonance is the smallest (16 ppm). The FWHM of the O<sup>44</sup> resonance is characterized by an intermediate value of  $\sim 27-28$  ppm. The FWHM, indicative of the chemical shift dispersion

of these resonances in the <sup>17</sup>O MAS NMR spectra, is likely a manifestation of the structural disorder in the bonding environment of the corresponding oxygen species. Therefore, it may be argued that the increasing concentration of high-coordinated Ge atoms in these glasses upon progressive addition of Na<sub>2</sub>O to GeO<sub>2</sub> to at least up to 18 mol% leads to increasing short-range structural disorder.

It was noted in previous studies that the resonance centered near ~90 ppm in the <sup>17</sup>O NMR spectra of these glasses cannot be uniquely assigned a priori to either O<sup>45</sup> or O<sup>46</sup> environments, as an experimental determination of the  $\delta_{iso}$  for the former has remained elusive due to the absence of such oxygen environment in known crystalline germanate phases. Moreover, the experimental  $\delta_{iso}$  for the O<sup>46</sup> environment covers a rather broad range of 80-150 ppm in crystalline sodium germanates. On the other hand, density functional theory-based calculations on small Nagermanate clusters have indicated that the difference between the  $^{17}O$   $\delta_{iso}$  for the  $O^{44}$  and  $O^{45}$ environments can range between 26 and 35 ppm, while that between O<sup>44</sup> and O<sup>46</sup> environments can range between 37 and 61 ppm [28]. Therefore, when taken together, the experimental  $\delta_{iso}$  of the  $O^{45/46}$  environment (~ 90 ppm) and its difference of ~ 40 ppm from that of the  $O^{44}$  environment suggest that the resonance at  $\sim 90$  ppm likely corresponds to the  $O^{46}$  environment. Further insight into this problem can be gained by estimating the average Ge-O coordination number from the oxygen speciation as evidenced in the <sup>17</sup>O MAS NMR spectra (Figure 2, Table 1). For a glass of composition  $(Na_2O)_x$  (GeO<sub>2</sub>)<sub>100-x</sub> the total number of oxygen atoms in the formula unit is: 200-x. If y is the relative fraction of oxygen atoms in  $O^{45/46}$  environment, then the number of oxygen atoms in this configuration is: y\*(200-x). If all of these oxygen atoms are of the type  $O^{46}$  i.e. high-coordinated Ge atoms are only of the type  $Ge^{VI}$ , and the  $Ge^{VI} \emptyset_{6/2}$  octahedra are interspersed with  $Ge^{IV} \emptyset_{4/2}$  tetrahedra such that these octahedra do not share any corner, then the total number

of  $Ge^{VI}$  atoms per formula unit is: y\*(200-x)/6, provided all bridging oxygen atoms are coordinated to two Ge atoms. The rest of the Ge atoms are obviously of the type  $Ge^{IV}$  and hence, the average Ge-O coordination number can be obtained from a simple weighted average of the number of  $Ge^{VI}$  and  $Ge^{IV}$  atoms in the formula unit. Similarly, if all high-coordinated Ge atoms in the structure were only of the type  $Ge^{V}$  then the total number of such atoms per formula units would simply be y\*(200-x)/5.

It may be noted that previous neutron scattering studies and the <sup>17</sup>O NMR results presented in this study indeed verify the validity of the two key assumptions made in these calculations: (i) all bridging oxygen are two-coordinated and (ii)  $Ge^{VI}\emptyset_{6/2}$  or  $Ge^{V}\emptyset_{5/2}$  polyhedra do not share corners with one another [4,11]. A rather minor violation of the second assumption is noted in the <sup>17</sup>O MAS NMR spectrum of the glass with x = 28, which indicates the presence of ~1% of the oxygen in the O<sup>666</sup> environment (Figure 2, Table 1). A comparison of the average Ge-O coordination numbers calculated following the abovementioned scheme with those obtained from previous neutron scattering experiments on  $(Na_2O)_x(GeO_2)_{100-x}$  glasses is shown in Figure 4, which displays a remarkable agreement only for the case of all high-coordinated Ge being present in these glasses as Ge<sup>VI</sup> species. This result clearly suggests that the O<sup>45/46</sup> resonance in the <sup>17</sup>O NMR spectra in Figure 2 can be ascribed predominantly to the presence of O<sup>46</sup> environments in these glasses. This preference of Ge to form Ge<sup>VI</sup> over Ge<sup>V</sup> is in clear contrast with that displayed by Al or Si, where the formation of fivefold coordinated AlV and SiV species almost invariably accompanies and often dominate over their sixfold coordinated counterparts in oxide glasses except perhaps in phosphosilicate glasses [31-35]. Therefore, such a preference of Ge for sixfold coordination with oxygen is unusual and its fundamental cause remains unclear at this stage. It may be noted here that previous Raman, Infrared and Ge K-edge EXAFS spectroscopic studies of  $(K_2O)_x$  (GeO<sub>2</sub>)<sub>100-x</sub> and  $(Rb_2O)_x$  (GeO<sub>2</sub>)<sub>100-x</sub> glasses by Jain and coworkers suggested a similar modification mechanism of the germanate network via the progressive conversion of Ge<sup>IV</sup> to Ge<sup>VI</sup> in compositions with up to  $x \approx 15$ -20 [36-38]. Finally, the compositional evolution of the average Ge-O coordination number in Fig. 4 and consequently the connectivity of the network go through a maximum near  $\sim 18$  mol% Na<sub>2</sub>O. The location of this maximum is consistent with the corresponding variation in the density of these glasses as shown in Fig. 1 as well as in their  $T_g$  as reported in the literature, both of which go through a maximum in the vicinity of this composition [8]. Therefore, when taken together, these results suggest a mechanistic connection between the germanate anomaly and the average Ge-O coordination number and connectivity of the network.

# 3.2. Fictive temperature dependence of glass structure

The <sup>17</sup>O MAS NMR spectra of the as-quenched and annealed  $(Na_2O)_x(GeO_2)_{100-x}$  glasses with, respectively, higher and lower  $T_f$  are compared in Figure 5 for compositions with x=18 and x=28. These spectra, when normalized to the O<sup>44</sup> resonance at ~ 50 ppm, clearly indicate that annealing below  $T_g$  and consequent lowering of  $T_f$  results in a relative increase in the intensity of the resonance near ~ 90 ppm. Therefore, in these glasses the ratio of  $Ge^{VI}/Ge^{IV}$  increases with decreasing  $T_f$ , which is indeed consistent with a concomitant increase in density (Figure 1). This result suggests a causal relationship between density and Ge-O coordination number, thus validating the key hypothesis of germanate anomaly.

Simulation of these <sup>17</sup>O MAS NMR spectra in Figure 4 indicates that for the glass with x = 18 the relative fraction of the O<sup>46</sup> species increased by 1.2% upon annealing at 490 °C for 7d (Table 2). On the other hand, in the case of the glass with x = 28, while the relative fraction of the O<sup>46</sup> species increased by 2.5%, that of the O<sup>44</sup> and the NBO species decreased by 1.5% and 1.2%,

respectively, upon annealing at 420 °C for 7d (Table 2). Finally, it is interesting to note that the relative fraction of the  $O^{666}$  species in this glass increased from 1.2% to 1.4% on annealing. Considering oxygen balance, such a change in oxygen speciation indeed suggests, within experimental error, a temperature dependence of the structural reaction in Eq. 3, which was proposed in a recent Raman spectroscopic study of  $K_2O$ -GeO<sub>2</sub> liquids [27]. This reaction shifts to the right with increasing temperature and is reminiscent of the well-known borate speciation reaction  $BO_4 = BO_3 + NBO$ , which has been established as a source of temperature dependent configurational entropy  $\frac{dS_{conf}}{dT}$  in borate liquids [25]. Therefore, it can be argued that, similar to borates, the apparently anomalous increase in fragility in germanate liquids with increasing connectivity upon initial addition of modifier alkali oxide to  $GeO_2$  is associated with the fact that network-forming cations such as B and Ge can assume multiple coordination environments with relative fractions that are sensitive to temperature [26].

#### 4. Conclusions

The analysis of the high-resolution  $^{17}O$  MAS NMR spectra presented here yields a comprehensive picture of the compositional evolution of structure and its temperature dependence in Na<sub>2</sub>O-GeO<sub>2</sub> glasses and liquids. When taken together, the NMR results indicate that initial addition of Na<sub>2</sub>O to GeO<sub>2</sub> to at least up to 18 mol% results in an increasing connectivity of the GeO network primarily via the formation of GeVI species. Further addition of Na<sub>2</sub>O results in a typical modification of the network i.e. a progressive loss of its connectivity as the NBO species appears and increases in concentration. This non-monotonic evolution of the connectivity of the network is consistent with the germanate anomaly in the corresponding compositional variation in density and  $T_g$  of these glasses. Finally, the germanate network in these glasses displays a temperature

dependent speciation equilibrium that can be schematically represented as:  $Ge^{VI} \leftrightarrow Ge^{IV}+NBO$ . This equilibrium shifts to the right with increasing temperature. Such speciation may act as a source of  $S_{conf}$  in supercooled germanate liquids and may provide an atomistic mechanism for viscous flow [39].

## **ACKNOWLEDGEMENTS**

This work is supported by the National Science Foundation Grant NSF DMR 1855176 to SS. The National High Magnetic Field Laboratory is supported by the National Science Foundation through NSF/DMR-1644779 and the State of Florida. The Development of the 36 T Series-Connected Hybrid magnet and NMR instrumentation was supported by NSF (DMR-1039938 and DMR-0603042) and NIH GM122698.

# **References:**

- [1] G. Greaves, S. Sen, Inorganic glasses, glass-forming liquids and amorphizing solids, Adv. Phys., 56 (2007) 1-166. https://doi.org/10.1080/00018730601147426.
- [2] A.K. Varshneya, J.C. Mauro, Fundamentals of inorganic glasses, third ed., Elsevier, New York, 2019.
- [3] J.F. Stebbins, J. Wu, L.M. Thompson, Interactions between network cation coordination and non-bridging oxygen abundance in oxide glasses and melts: Insights from NMR spectroscopy, Chem. Geol. 346, 34 (2013). https://doi.org/10.1016/j.chemgeo.2012.09.021
- [4] L.-S. Du, J.F. Stebbins, Oxygen Sites and Network Coordination in Sodium Germanate Glasses and Crystals: High-Resolution Oxygen-17 and Sodium-23 NMR, J. Phys. Chem. B **110**, 12427 (2006). https://doi.org/10.1021/jp0615510.
- [5] L. Peng, J.F. Stebbins, Sodium germanate glasses and crystals: NMR constraints on variation in structure with composition, J. Non-Cryst. Solids, 353, 4732 (2007). https://doi.org/10.1016/j.jnoncrysol.2007.06.066.
- [6] A.C. Hannon, D. Di Martino, L.F. Santos, R.M. Almeida, A model for the Ge–O coordination in germanate glasses, J. Non-Cryst. Solids, 353, 1688 (2007). https://doi.org/10.1016/j.jnoncrysol.2007.02.046.
- [7] G.S. Henderson, H.M. Wang, Germanium coordination and the germanate anomaly, Eur. J. Miner. 14, 733 (2002). https://doi.org/10.1127/0935-1221/2002/0014-0733.
- [8] T.J. Kiczenski, C. Ma, E. Hammarsten, D. Wilkerson, M. Affatigato, S. Feller, A study of selected physical properties of alkali germanate glasses over wide ranges of composition, J. Non-Cryst. Solids, 272, 57 (2000). https://doi.org/10.1016/S0022-3093(00)00158-7

- [9] T. Furukawa, W.B. White, Raman spectroscopic investigation of the structure and crystallization of binary alkali germanate glasses, J. Mater. Sci. 15, 1648 (1980). https://doi.org/10.1007/BF00550581.
- [10] A.C. Hannon, D. Di Martino, L.F. Santos, R.M. Almeida, Ge-O Coordination in Cesium Germanate Glasses, J. Phys. Chem. B, 111, 3342. (2007). https://doi.org/10.1021/jp066714z.
- [11] M. Ueno, M. Misawa, K. Suzuki, On the change in coordination of Ge atoms in Na2O GeO2 glassess, Physica B&C, 120, 347 (1983). https://doi.org/10.1016/0378-4363(83)90404-7.
- [12] U. Hoppe, R. Kranold, H.-J. Weber, J. Neuefeind, A.C. Hannon, The structure of potassium germanate glasses a combined X-ray and neutron scattering study, J. Non-Cryst. Solids, 278, 99 (2000). https://doi.org/10.1016/S0022-3093(00)00333-1.
- [13] W.C. Huang, H. Jain, G. Meitzner, The structure of potassium germanate glasses by EXAFS, J. Non-Cryst. Solids, 196, 155 (1996). https://doi.org/10.1016/0022-3093(95)00578-1.
- [14] G.S. Henderson, M.E. Fleet, The structure of glasses along the Na2O GeO2 join, J. Non-Cryst. Solids, 134, 259 (1991). https://doi.org/10.1016/0022-3093(91)90384-I.
- [15] H.M. Wang, G.S. Henderson, Investigation of coordination number in silicate and germanate glasses using O K-edge X-ray absorption spectroscopy, Chem. Geol., 213, 17 (2004). https://doi.org/10.1016/j.chemgeo.2004.08.029
- [16] H.M. Wang, G.S. Henderson, The germanate anomaly: Is the presence of five- or six-fold Ge important?, Phys. Chem. Glasses, 46, 377 (2005).
- [17] P. Ghigna, P. Mustarelli, C. Tomasi, E. Quartarone, M. Scavini, A. Speghini, M. Bettinelli, A Combined Nuclear Magnetic Resonance and X-ray Absorption Fine Structure Study on the Local Structures of Ge and Pb in PbO–GeO2 Glasses and Their Relationships with Thermal

- Properties and Devitrification Products, J. Phys. Chem. B 106, 9802 (2002). https://doi.org/10.1021/jp026133j.
- [18] E.F. Riebling, Structure of Molten Oxides. II. A Density Study of Binary Germanates Containing Li2O, Na2O, K2O, and Rb2O, J. Phys. Chem., 39, 3022 (1963). https://doi.org/10.1063/1.1734137.
- [19] J.F. Stebbins, S.E. Ellsworth, Temperature Effects on Structure and Dynamics in Borate and Borosilicate Liquids: High-Resolution and High-Temperature NMR Results, J. Am. Ceram. Soc. **79**, 2247 (1996). https://doi.org/10.1111/j.1151-2916.1996.tb08969.x.
- [20] S. Sen, Z. Xu, J.F. Stebbins, Temperature dependent structural changes in borate, borosilicate and boroaluminate liquids: high-resolution 11B, 29Si and 27Al NMR studies, J. Non. Cryst. Solids **226**, 29 (1998). https://doi.org/10.1016/S0022-3093(97)00491-2.
- [21] S. Sen, Temperature induced structural changes and transport mechanisms in borate, borosilicate and boroaluminate liquids: high-resolution and high-temperature NMR results, J. Non. Cryst. Solids 253, 84 (1999). https://doi.org/10.1016/S0022-3093(99)00346-4.
- [22] L. Cormier, O. Majérus, D.R. Neuville, G. Calas, Temperature-Induced Structural Modifications Between Alkali Borate Glasses and Melts, J. Am. Ceram. Soc. **89**, 13 (2006). https://doi.org/10.1111/j.1551-2916.2005.00657.x.
- [23] O. Majérus, L. Cormier, G. Calas, B. Beuneu, Temperature-induced boron coordination change in alkali borate glasses and melts, Phys. Rev. B **67**, 024210 (2003). https://doi.org/10.1103/PhysRevB.67.024210.
- [24] O.L. Alderman, C.J. Benmore, A. Lin, A. Tamalonis, J.R. Weber, Borate melt structure: Temperature-dependent B–O bond lengths and coordination numbers from high-energy X-ray diffraction, J. Am. Ceram. Soc., 101 (2018) 3357-3371. https://doi.org/10.1111/jace.15529.

- [25] O.L. Alderman, C.J. Benmore, B. Reynolds, B. Royle, S. Feller, J.R. Weber, Liquid fragility maximum in lithium borate glass-forming melts related to the local structure, Int. J. Appl. Glass Sci., (2022). https://doi.org/10.1111/ijag.16611.
- [26] S. Sen, H. Chen, Sources of Configurational Entropy versus Compositional Trends in Fragility of Inorganic Glass-Forming Liquids, Phys. Stat. Sol. B, 259, 2200002 (2022). https://doi.org/10.1002/pssb.202200002.
- [27] O.N. Koroleva, A.A. Osipov, In situ Raman spectroscopy of K2O-GeO2 melts, J. Non. Cryst. Solids **531**, 119850 (2020). https://doi.org/10.1016/j.jnoncrysol.2019.119850.
- [28] S.K. Lee, B.H. Lee, Atomistic Origin of Germanate Anomaly in GeO2 and Na-Germanate Glasses: Insights from Two-Dimensional 17O NMR and Quantum Chemical Calculations, J. phys. Chem. B, 110, 16408 (2006). https://doi.org/10.1021/jp063847b.
- [29] D. Massiot, V. Montouillout, C. Bessada, J.P. Coutures, H. Forster, S. Steuernagel, D. Muller, C.R. Acad. Towards higher resolution for quadrupolar nuclei in solid state NMR at very high fieldVers une plus haute résolution pour les noyaux quadripolaires en RMN du solide à très hauts champs, Sci. Paris, IIc, 157 (1998). https://doi.org/10.1016/S1387-1609(99)80074-7.
- [30] Z. Gan, P. Gor'kov, T.A. Cross, A. Samoson, D. Massiot, Seeking Higher Resolution and Sensitivity for NMR of Quadrupolar Nuclei at Ultrahigh Magnetic Fields, J. Am. Chem. Soc., 124, 5634 (2002). https://doi.org/10.1021/ja025849p.
- [31] D.R. Neuville, L.Cormier, V. Montouillout, P. Florian, F. Millot, J.C. Rifflet, D. Massiot, Amorphous materials: Properties, structure, and durability†: Structure of Mg- and Mg/Ca aluminosilicate glasses: 27Al NMR and Raman spectroscopy investigations, American Mineralogist, 93, 1721-31 (2008). https://doi.org/10.2138/am.2008.2867.

- [32] S Sen, Z Xu, J.F Stebbins, Temperature dependent structural changes in borate, borosilicate and boroaluminate liquids: high-resolution 11B, 29Si and 27Al NMR studies, J. Non-Cryst. Solids, 226, 29-40 (1998). https://doi.org/10.1016/S0022-3093(97)00491-2.
- [33] S. J. Gaudio, C. E. Lesher, H. Maekawa, S. Sen, Geochim. Linking high-pressure structure and density of albite liquid near the glass transition, Cosmochim. Acta, 157, 28-38 (2015). https://doi.org/10.1016/j.gca.2015.02.017.
- [34] J. F. Stebbins, I. Farnan, X. Xue, The structure and dynamics of alkali silicate liquids: A view from NMR spectroscopy, Chem. Geol., 96, 371 (1992). https://doi.org/10.1016/0009-2541(92)90066-E
- [35] J. Ren, H. Eckert, Superstructural Units Involving Six-Coordinated Silicon in Sodium Phosphosilicate Glasses Detected by Solid-State NMR Spectroscopy, J. Phys. Chem. C, 122, 27620 (2018). https://doi.org/10.1021/acs.jpcc.8b09779.
- [36] E.I. Kamitsos, Y.D. Yiannopoulos, M.A. Krakassides, G.D. Chryssikos, H. Jain, Raman and Infrared Structural Investigation of xRb2O·(1 x)GeO2 Glasses, J. Phys. Chem., 100, 11755-11765 (1996). https://doi.org/10.1021/jp960434+.
- [37] W.C. Huang, H. Jain, M.A. Marcus, Structural study of Rb and (Rb,Ag) germanate glasses by EXAFS and XPS, J. Non-Cryst. Solids, 180, 40 (1994). https://doi.org/10.1016/0022-3093(94)90395-6.
- [38] Y.D. Yiannopoulos, E.I. Kamitsos, H. Jain, In: Andriesh, A., Bertolotti, M. (eds) Physics and Applications of Non-Crystalline Semiconductors in Optoelectronics. NATO ASI Series, vol 36. pp. 317-325, Springer, Dordrecht.
- [39] S. Sen, Dynamics in inorganic glass-forming liquids by NMR spectroscopy, Prog. NMR Spectroscopy, 116, 155-176 (2020). https://doi.org/10.1016/j.pnmrs.2019.11.001.

**Table 1.** <sup>17</sup>O MAS NMR spectral simulation parameters for spectra of as-quenched  $(Na_2O)_x$   $(GeO_2)_{100-x}$  glasses collected at 35.2 T.

(Na <sub>2</sub> O) <sub>x</sub> (GeO <sub>2</sub> ) <sub>100-x</sub> Glass composition	sites	$\delta_{iso}$ (ppm)	width (ppm)	Relative fraction (±1.5%)
<i>x</i> = 4	O <sup>44</sup>	43	26	85%
	O <sup>45/46</sup>	83	40	15%
<i>x</i> = 8	O <sup>44</sup>	47	28	70%
	O <sup>45/46</sup>	86	45	30%
x = 18	O <sup>44</sup>	55	28	48.2%
	O <sup>45/46</sup>	92	48	51.8%
x = 28	O <sup>44</sup>	61	24	50.8%
	O <sup>45/46</sup>	93	37	28.3%
	NBO	44	20	19.7%
	O <sup>666</sup>	237	16	1.2%

**Table 2.**  $^{17}O$  MAS NMR spectral simulation parameters for spectra of as-quenched vs. annealed  $(Na_2O)_x(GeO_2)_{100-x}$  glasses collected at 35.2 T.

(Na <sub>2</sub> O) <sub>x</sub> (GeO <sub>2</sub> ) <sub>100-x</sub> Glass composition	sites	$\delta_{iso}$ (ppm)	width (ppm)	*Relative fraction
<i>x</i> = 18	O <sup>44</sup>	55	28	48.2%
Quenched	O <sup>45/46</sup>	92	48	51.8%
<i>x</i> = 18	O <sup>44</sup>	55	28	47%
Annealed	O <sup>45/46</sup>	92	48	53%
	O <sup>44</sup>	61	24	50.8%
x = 28	O <sup>45/46</sup>	93	37	28.3%
Quenched	NBO	44	20	19.7
	O <sup>666</sup>	237	16	1.2
	O <sup>44</sup>	61	24	49.3%
x = 28	O <sup>45/46</sup>	93	37	30.8%
Annealed	NBO	44	20	18.5
	O <sup>666</sup>	237	16	1.4

<sup>\*</sup>For each glass composition relative variation between the site fractions obtained in simulations for quenched and annealed samples is  $\pm 0.5\%$  or less.

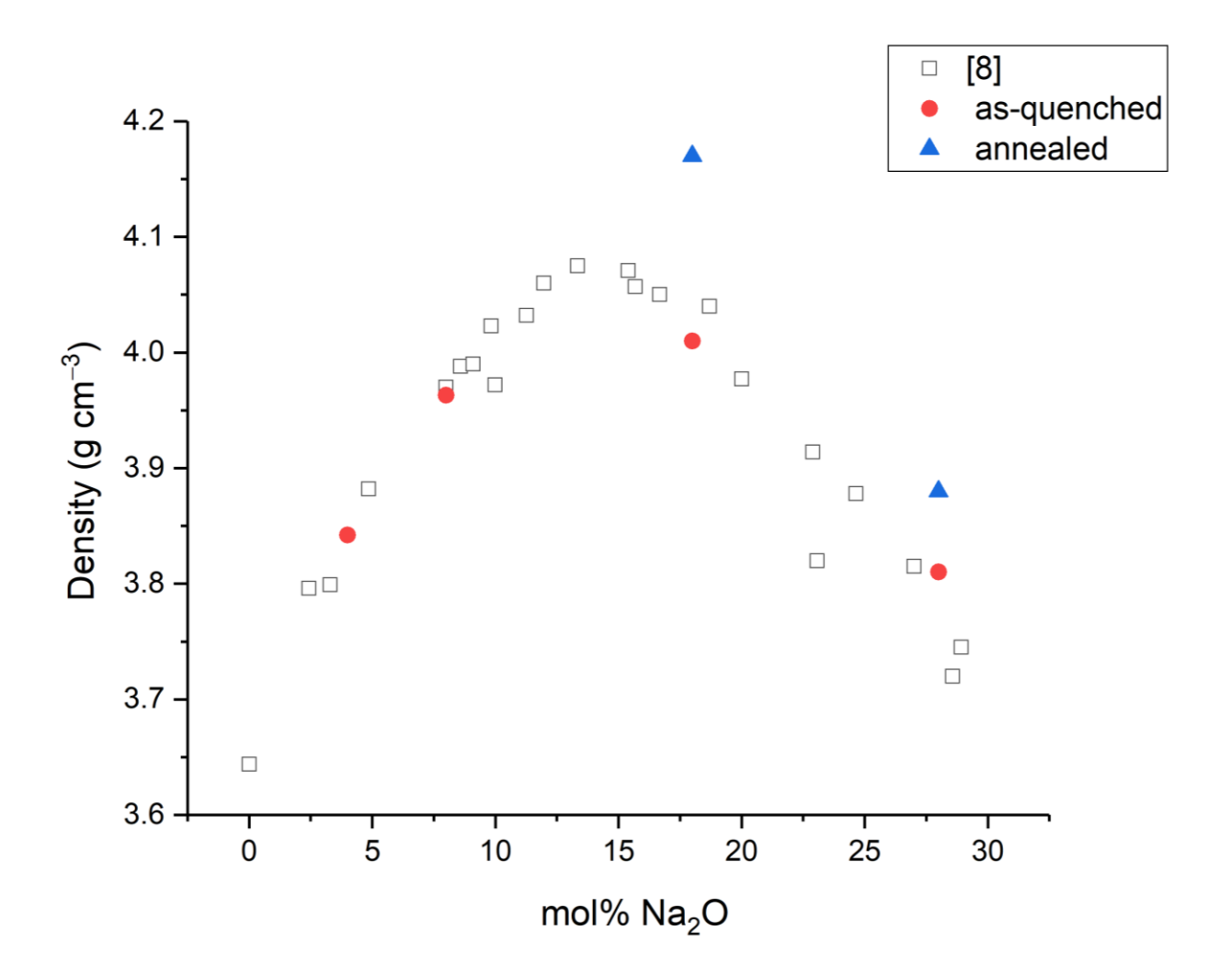


**Fig. 1.** Composition dependence of density of as-quenched  $(Na_2O)_x(GeO_2)_{100-x}$  glasses (red circles) and for glasses with 18 and 28 mol%  $Na_2O$  after annealing (blue triangles). Density of  $(Na_2O)_x$   $(GeO_2)_{100-x}$  glasses reported in the literature (open squares) is shown for comparison [8].

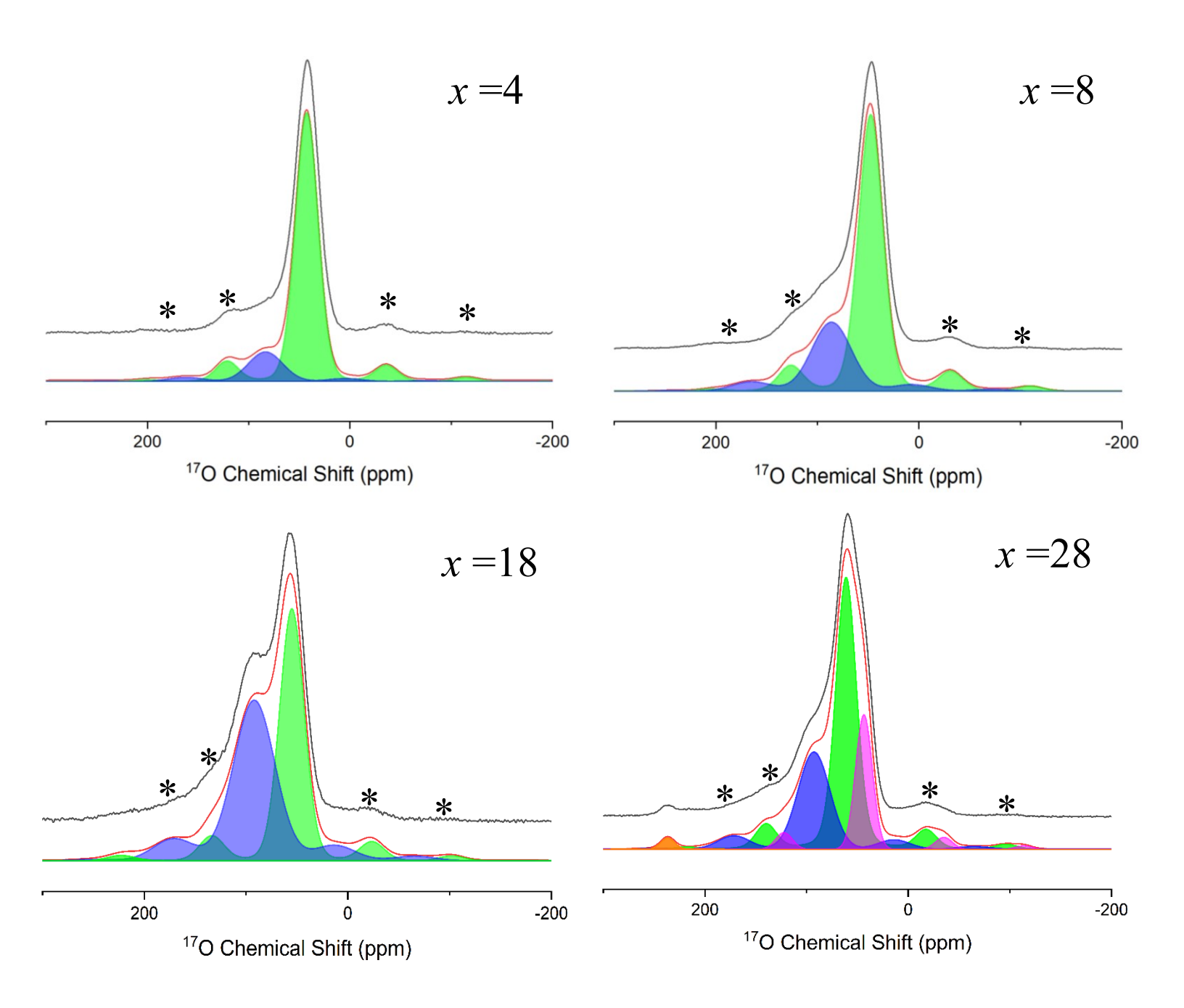


**Fig. 2.** Experimental (black solid line) and simulated (solid red line)  $^{17}O$  MAS NMR spectra of asquenched (Na<sub>2</sub>O)<sub>x</sub> (GeO<sub>2</sub>)<sub>100-x</sub> glasses with compositions given alongside the spectra. Asterisks denote spinning sidebands. Center band and spinning sidebands of individual simulation components for  $O^{44}$ ,  $O^{45/46}$ , NBO and  $O^{666}$  sites are shown in green, blue, pink and orange, respectively.

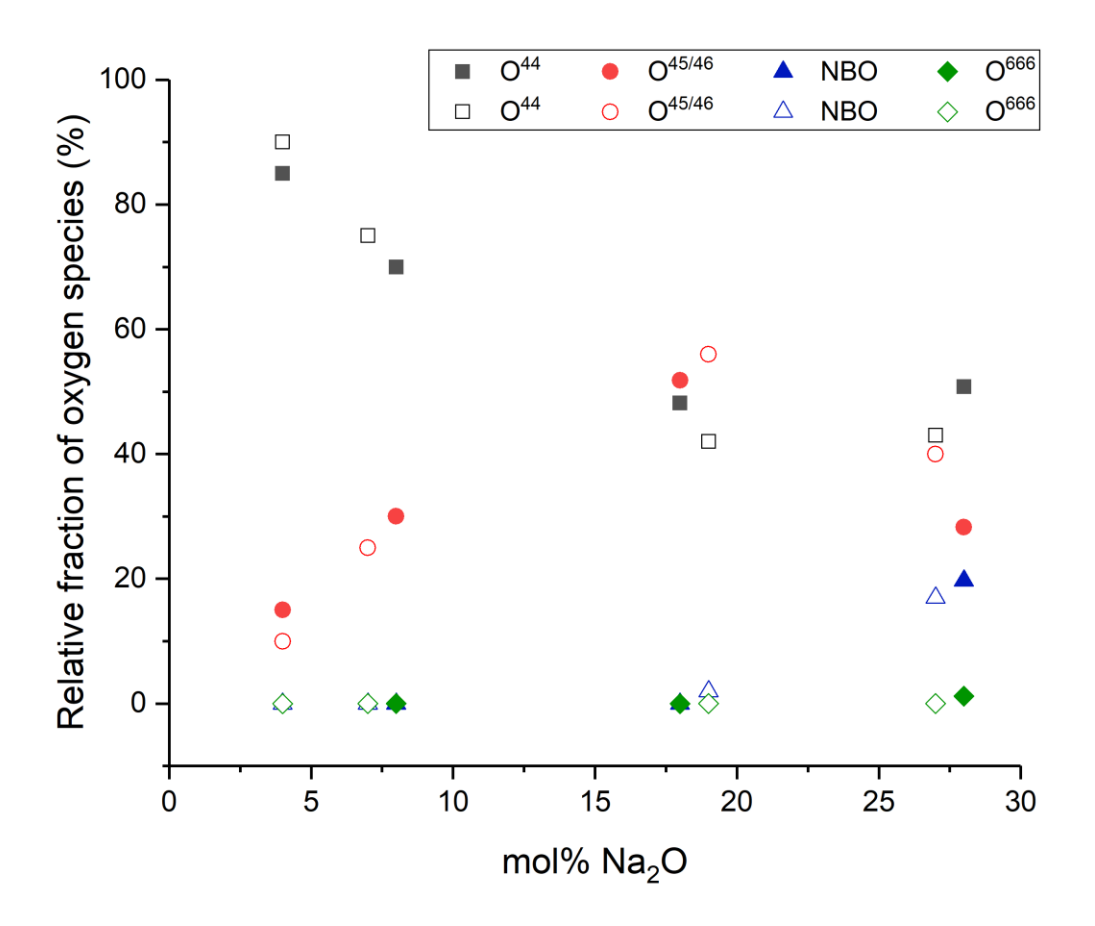


**Fig. 3.** Compositional variation of the relative fraction of various oxygen species in as-quenched  $(Na_2O)_x(GeO_2)_{100-x}$  glasses (filled symbols) as estimated in this study from simulation of ultrahigh field <sup>17</sup>O MAS NMR spectra and those obtained from <sup>17</sup>O 3QMAS NMR spectra [5] for comparable compositions (open symbols). The experimental error bar for the filled symbols is on the order of  $\pm 1.5\%$  and range between  $\pm 3\%$  and  $\pm 6\%$  for the open symbols.

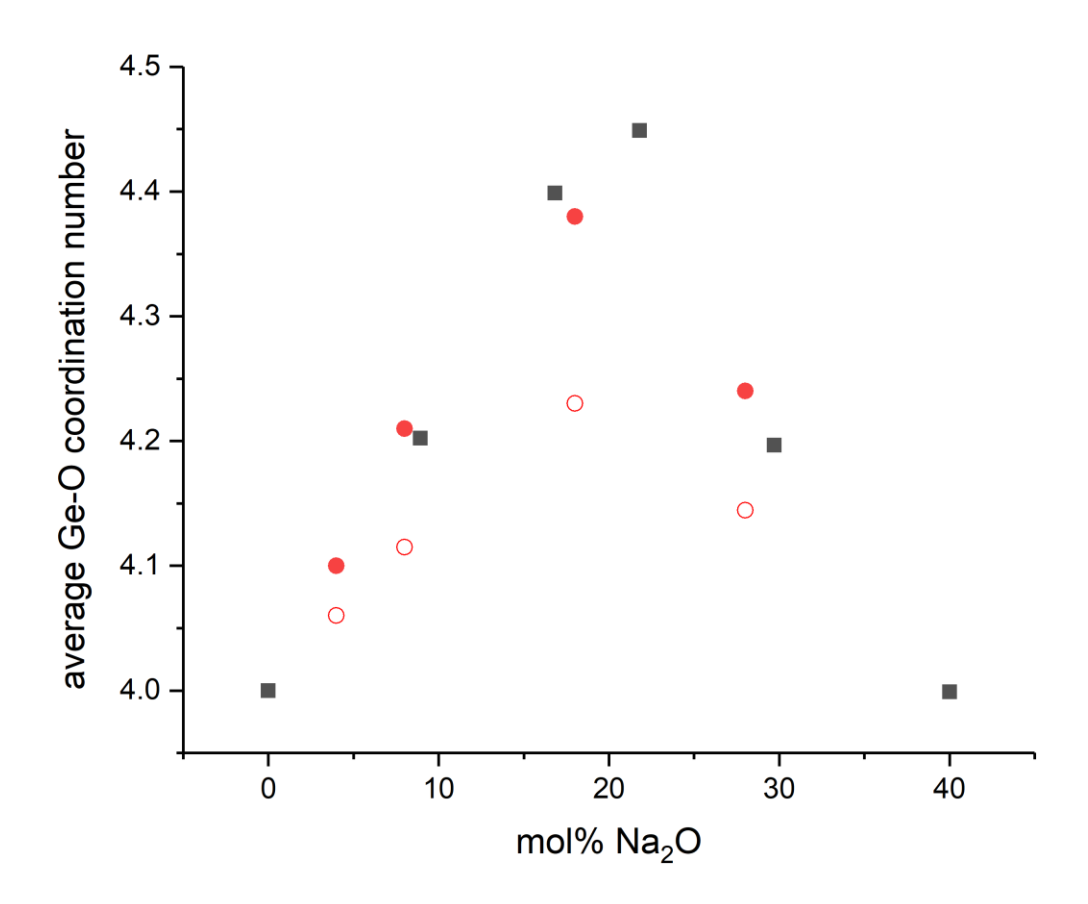


**Fig. 4.** Average Ge-O coordination number of as-quenched  $(Na_2O)_x$  (GeO<sub>2</sub>)<sub>100-x</sub> glasses estimated from <sup>17</sup>O NMR-based oxygen speciation under the assumption of all high-coordinated Ge atoms being present as  $Ge^{VI}$  (filled circles) and as  $Ge^{V}$  (open circles). Average Ge-O coordination number of  $(Na_2O)_x$  (GeO<sub>2</sub>)<sub>100-x</sub> glasses determined in a previous study by neutron scattering (filled squares) is shown for comparison [11].

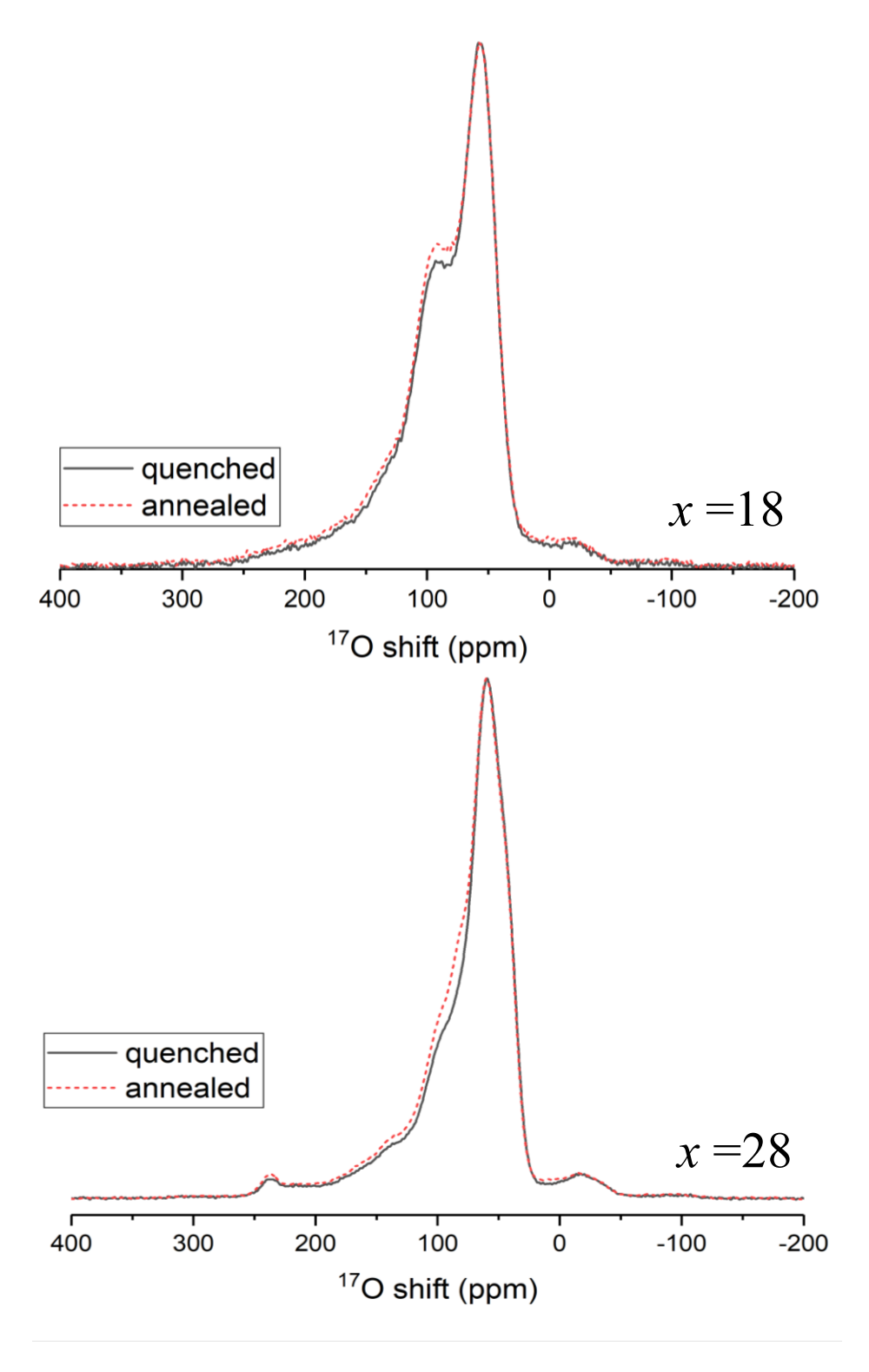


**Fig. 5.** <sup>17</sup>O MAS NMR spectra of as-quenched (solid black line) and annealed (dashed red line)  $(Na_2O)_x(GeO_2)_{100-x}$  glasses with compositions given alongside the spectra.